Current Optics and Photonics
Vol. 1, No. 2, April 2017, pp. 157-162

ISSN: 2508-7266(Print) / ISSN: 2508-7274(Online)
DOI: https://doi.org/10.3807/COPP.2017.1.2.157

Reduction of Gamma Distortion in Oblique Viewing Directions in Polymer-stabilized Vertical Alignment Liquid Crystal Mode

Hyo Joong Kim[1], Young Jin Lim[1], G. Murali[1], Min Su Kim[1,2], Gi Heon Kim[3], Yong Hae Kim[3], Gi-Dong Lee[4]*, and Seung Hee Lee[1]**

[1]*Applied Materials Institute for BIN Convergence, Department of BIN Convergence Technology and Department of Polymer-Nano Science and Technology, Chonbuk National University, Jeonju, Jeonbuk 54896, Korea*
[2]*Liquid Crystal Institute, Kent State University, Kent, OH 44242, USA*
[3]*Electronics and Telecommunications Research Institute, Daejeon 34129, Korea*
[4]*Department of Electronics Engineering, Dong-A University, Busan 49315, Korea*

(Received November 8, 2016 : revised December 12, 2016 : accepted February 7, 2017)

In large liquid crystal displays, the image quality in an oblique viewing direction is a crucial issue. From this perspective, 8-domain polymer-stabilized vertical alignment (PS-VA) mode has been developed to suppress the color shift in oblique viewing directions, compared to that in 4-domain PS-VA mode. To realize the 8-domain PS-VA, the four domains in a pixel are each divided into two regions, such that applying different electric potentials result in different tilt angles in these two regions, while keeping four azimuthal directions in each domain. However, applying different voltages in a pixel causes drawbacks, such as requiring additional processes to construct a capacitor and a transistor, which will further reduce the aperture ratio. Here we propose a different approach to form the 8-domain, by controlling surface polar anchoring energy and the width of patterned electrodes in two regions of a pixel. As a result, the gamma-distortion index (*GDI*), measured at an azimuthal angle of 0°, is reduced by about 23% and 8%, compared to that of a conventional 4-domain at polar angles of 30° and 60° respectively.

Keywords : Liquid crystal display, Vertical alignment, 8-domain, Color shift
OCIS codes : (230.2090) Electro-optical devices; (230.3720) Liquid-crystal devices

I. INTRODUCTION

Liquid crystal displays (LCDs) have been dominating flat-panel display markets for a long time, because extensive research has long been performed to drop the cost and enhance the image quality. Spontaneously, many liquid crystal (LC) modes have been proposed, such as in-plane switching (IPS) [1, 2], fringing field switching (FFS) [3-5], and vertical -alignment (VA) modes [6, 7]. Among these modes, the VA mode has been widely used in LCD television (TV), due to its advantageous electro-optic properties, such as fast response time and high contrast ratio in the normal direction. On the other hand, a few unsolved drawbacks remain, such as color shift and gamma distortion, which originate from the initially vertical alignment. Many works have been reported to overcome such drawbacks with their own particular features, *e.g.* multidomain vertical alignment (MVA), which has protrusions on the surface [8, 9]; advanced super-view (ASV) [10]; patterned vertical alignment (PVA), which utilizes an oblique electric field formed by electrodes of desired patterns [11-13]; and polymer-stabilized vertical alignment (PS-VA), in which a pretilt angle is achieved by a certain polymer morphology on the surface [14-16]. In all VA modes, vertically aligned LCs tilt down in four different azimuthal directions, to improve the viewing-angle property. However, retardation of the LC layer causes a color shift as the viewing angle changes from normal to oblique [17]. As a result, the

*Corresponding author: *gdlee@dau.ac.kr, **lsh1@chonbuk.ac.kr
Color versions of one or more of the figures in this paper are available online.

viewing-angle property was further improved by dividing each pixel into two regions, to produce different voltages, which can give rise to different LC behavior in each region [18-22]. According to the driving method, the 8-domain mode can be classified according to many types:, including the capacitor-coupling type (C-C Type), which can generate different voltages for each domain by adding a capacitor [23], and the two-transistor type (T-T Type), which independently controls the voltages in desired regions [21, 24]. More recently, the charge-shared type (CS Type) was proposed, in which upper and lower adjacent pixels are charged simultaneously using one-gate two-data [22] or half-gate two-data [25], and also the resistivity-division type (RD Type) [26] was reported, in which a pixel is divided into high-pixel (high-tilt-angle zone) and low-pixel (low-tilt-angle zone), without extra sharing gate lines and additional data lines. However, all of the technologies mentioned above give rise to reduced aperture ratio, due to the additional data lines and transistors in the 8-domain mode.

To overcome these drawbacks, here we propose a novel method to form 8-domains by controlling the width and space of electrodes in both main regions and subregions, in combination with the polar anchoring strength.

II. SWITCHING PRINCIPLE AND SIMULATION CONDITIONS OF THE PROPOSED 8-DOMAIN PS-VA MODE

The normalized transmission of light through the VA cell in which a vertically aligned uniaxial LC medium is driven by an oblique electric field under a crossed polarizer is given by

$$T/T_0 = sin^2(2\psi(V))sin^2(\pi d\Delta n_{eff}(V)/\lambda) \quad (1)$$

where ψ is the voltage-dependent angle between one of the transmittance axes of the crossed polarizers and the LC director; d is the cell gap; Δn_{eff} is the effective birefringence of the LC medium, dependent on voltage and viewing angle (θ = polar angle, ϕ = azimuthal angle); and λ is the wavelength of incident light. In the PS-VA mode, the LC director is initially vertically aligned, but an extra process such as polymer stabilization under an electric field is performed to give a pretilt angle of about 89° in four ϕs. In the voltage-off state, an excellent dark state is achieved, due to the very small value of Δn_{eff}. In the voltage-on state, ψ (V) should be 45° and $d\Delta n_{eff}$ (V) should be $\lambda/2$, to achieve maximum transmittance in the normal direction. In addition, the LC director should reorient in four azimuthal directions, to minimize the viewing-angle dependence of the $d\Delta n_{eff}$ in 4-domain PS-VA mode. Nevertheless, quite strong color shift of the image as displayed in the normal direction does occur for oblique viewing directions of the 4-domain device, because $d\Delta n_{eff}$ changes abruptly as θ increases at a fixed ϕ [20]. To

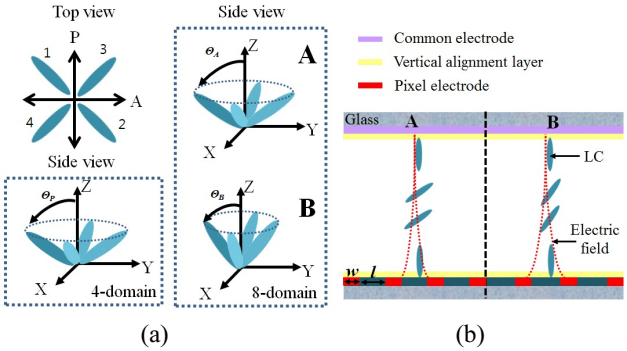

FIG. 1. (a) Configuration of LC directors in on-state of the 4-domain and 8-domain VA modes, and (b) side-view of fishbone electrode structure, indicating that the tilt angle of the LC director in region A is smaller than in region B, due to difference in field intensity, though the same voltage is applied to both regions.

reduce such a color shift, an 8-domain VA mode is proposed, in which one pixel is divided into two regions and the LC director in each region has two different tilt angles, low-tilt angle θ_A and high-tilt angle θ_B, while keeping a 4-domain in each region, as shown in Fig. 1(a).

The reorientation of vertically aligned LCs is determined by competition between the elastic energy of the LC cell and the applied electric field. In two regions of the device, the same LC is filled so that the field response to the LC in each region is the same. On the other hand, the magnitude of the anchoring energy, especially the polar anchoring energy W_θ, can determine the tilt angle of the LC director at a given voltage, because the main deformation of LCs is associated with bending [27, 28] and also the field intensity determines the tilt angle of the LC director. In PS-VA mode, the pixel electrode is patterned like a fishbone [29] with electrode width w and distance l between electrodes, as shown in Fig. 1(b). When the l in region A is different than that in the region B, the average field intensity that the LCs experience is different; that is, the narrower l is, the higher the field intensity becomes, such that the tilt angle of the LC director in region A can be smaller than that in the region B, though the same voltage is applied to both regions.

To test the feasibility of the proposed 8-domain PS-VA mode, we used a three-dimensional simulation program (TechWiz LCD, SANAYI system Co., Korea) to simulate the electro-optical properties of the proposed structures. The following conditions were set for the simulation: the negative dielectric anisotropy $\Delta\varepsilon$ = -4, and the birefringence Δn = 0.0816 at 589.3 nm. The surface pretilt angle was 89° (in experiment, this can be achieved by curing a reactive monomer in the PS-VA mode [15-17]), and d was 4 μm. Planar indium tin oxide (ITO) and fishbone-shaped ITO electrodes were used on the top and bottom substrates respectively. The pitch of the patterned electrode in each domain was kept constant while w and l in the fishbone-

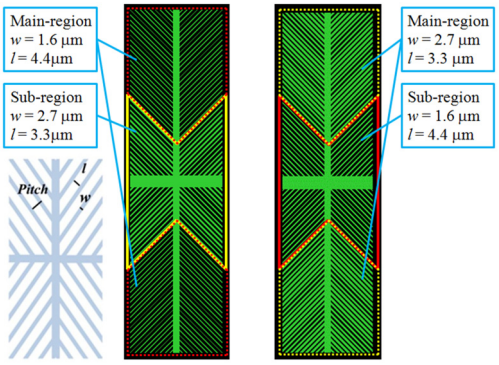

(a) (b)

FIG. 2. Top view of fishbone-shaped electrode with different electrode width and distances between electrodes in two regions of a pixel: (a) Cases 1 and 2; (b) Case 3.

TABLE 1. Simulation conditions for the proposed 8-domain PS-VA mode

Cases		w [μm]	l [μm]	W_θ [N/m]	W_φ [N/m]
Case 1	Main	1.6	4.4	10^{-3}	10^{-3}
	Sub	2.7	3.3	10^{-3}	10^{-3}
Case 2	Main	1.6	4.4	10^{-3}	10^{-3}
	Sub	2.7	3.3	10^{-4}	10^{-3}
Case 3	Main	2.7	3.3	10^{-4}	10^{-3}
	Sub	1.6	4.4	10^{-3}	10^{-3}

shaped electrodes varied, as shown in Fig. 2. For the 8-domain PS-VA mode, a pixel was divided into a main region and subregions, and the simulation was done in three sets: cases 1, 2, and 3, as shown in Table 1. In both cases 1 and 2 the same electrode structures were set as w (l) = 1.6 (4.4) μm in the main region and w (l) = 2.7 (3.3) μm in each subregion, as shown in Fig. 2(a), while the electrode structures in the main and subregions were interchanged in case 3, as shown in Fig. 2(b). For the anchoring conditions, in case 1 both W_θ and azimuthal W_φ anchoring energies were 10^{-3} N/m, representing strong anchoring conditions [30]. In case 2, the polar anchoring energy was set differently as W_θ = 10^{-3} N/m and 10^{-4} N/m in main and subregions respectively, while the azimuthal anchoring energy was the same in both regions, W_φ = 10^{-3} N/m. Finally, in case 3 the anchoring energies were also interchanged between main and subregions. In all cases the ratio of the main-region to sub-regions was 2:1.

III. RESULTS AND DISCUSSION

We first simulated the voltage-dependent transmittance (V-T) of the conventional 4-domain with respect to the electrode width and space, and to the magnitude of W_θ at

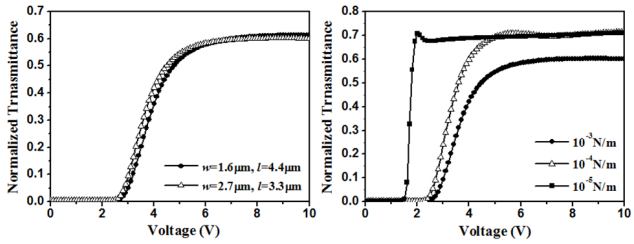

(a) (b)

FIG. 3. Voltage-dependent transmittance curves (a) with respect to w and l at $W_\theta = W_\varphi = 10^{-3}$ N/m, and (b) with respect to magnitude of W_θ at w (l) = 2.7 (3.3) μm in the conventional 4-domain case.

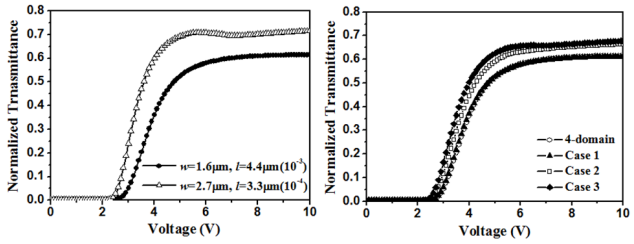

(a) (b)

FIG. 4. Voltage-dependent transmittance curves (a) for two different sets of (w, l, W_θ) in the conventional 4-domain case, and (b) for the conventional 4-domain case with w (l) = 1.6 (4.4) μm and $W_\theta = 10^{-3}$ N/m, and the three-proposed 8-domain cases.

fixed W_φ, as shown in Fig. 3. In experiment, the anchoring energies of the alignment layer can be controlled by the degree of polymerization of a monomer in the PS-VA mode, and also by mixing planar and vertical alignment materials in the same layer [17]. As shown in Fig. 3(a), the threshold voltage V_{th}, which is defined as a 10% transmittance change from a dark state, is 2.9 V and 3.0 V at W_θ = W_φ = 10^{-3} N/m with l = 3.3 μm and l = 4.4 μm respectively. The fact that V_{th} with l = 3.3 μm is 0.1 V lower than that with l = 4.4 μm indicates that the narrower electrode spacing can contribute to a stronger vertical component of an applied electric field, giving rise to lower V_{th}. The V-T curves at w = 2.7 μm and l = 3.3 μm with different magnitudes of W_θ also reveal that lower anchoring energy results in lower V_{th} and lower operating voltage V_{op}, as shown in Fig. 3(b).

After confirming that the V-T curves are strongly related to electrode structure and the magnitudes of anchoring energies, we changed W_θ = 10^{-4} N/m in the region with w (l) = 2.7 (3.3) μm, while keeping W_θ = 10^{-3} N/m in the region with w (l) = 1.6 (4.4) μm, and then V-T curves were calculated as shown in Fig. 4(a). Here the magnitude of W_φ was fixed. As expected, V_{th} is lowered by 0.4 V at W_θ = 10^{-4} N/m in the region with w (l) = 2.7 (3.3) μm, and also higher transmittance is observed. Based on this

result, we designed the following four different cases, including cases 1, 2, and 3 introduced in Table 1, and tested the electro-optic performance. One additional case is the conventional 4-domain structure with w (l) = 1.6 (4.4) μm and W_θ = 10^{-3} N/m. Figure 4(b) shows V-T curves for all four cases. The V-T curves of the conventional 4-domain case and case 1 exhibit similar behavior with V_{th} = 3 V, while the V-T curves of cases 2 and 3 show lower V_{th} of 2.8 V and 2.7 V respectively, and higher transmittance of 8.1% and 10.4% respectively, owing to relatively weak polar anchoring energy.

Figure 5 shows the pixel images in grayscale for all four cases. Cases 2 and 3 clearly exhibit a difference in transmittance between the two regions, and case 1 is relatively difficult to distinguish, especially at high transmittance. This indicates that the deviation of the tilt angle between two regions is greater in cases 2 and 3 than in case 1.

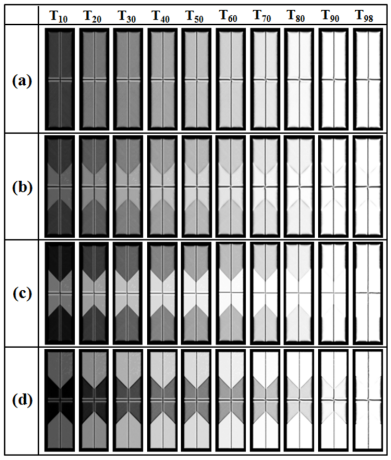

FIG. 5. The luminance of pixels in several gray levels for (a) The conventional 4-domain case, (b) Case 1, (c) Case 2, and (d) Case 3.

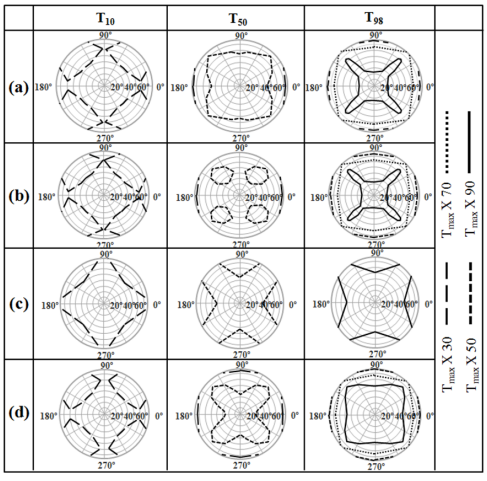

FIG. 6. Isoluminance curves at several gray values (T_{10}, T_{50} and T_{98}) in (a) The conventional 4-domain case, (b) Case 1, (c) Case 2, and (d) Case 3.

Figure 6 shows the isoluminance curves at different grayscale values in each case (T_{10}, T_{50} and T_{98}; here the numbers in subscripts indicate relative transmittance with respect to maximal transmittance). Here the isoluminance curves are normalized to the maximal luminance in case 3 in the normal viewing direction, and the relative luminances 90%, 70%, 50%, and 30% are indicated by a solid line and the various dotted lines, as shown in the last column to the right. As shown in the first column for T_{10} in Fig. 6, relative luminance of less than 30% exists within a polar angle of 40° in diagonal directions for the conventional 4-domain, cases 1 and 3, whereas it exists within a polar angle of 50° for case 2. In the third column for T98 in Fig. 6(c), remarkably, a relative luminance of 90% exists above a polar angle of 50° in every azimuthal direction in case 2. This indicates that case 2 shows the least luminance change, that is, wide viewing angle among all cases according to viewing angle changes.

In Fig. 7 are plotted the gamma curves, with a gamma correction factor following the power law γ = 2.2, for various viewing directions [31]. To simplify comparison, the azimuthal angle 0°, which is coincident with the transmittance axis of one of the polarizers, is fixed, while changing the polar angle from 0° to 60°. As clearly shown in the plots, the gamma curves in the conventional 4-domain case and cases 1 and 3 exhibit grayscale inversion upon changing the viewing direction. Unlike the others, case 2 shows the best characteristic with respect to gamma distortion among all cases. To investigate this quantitatively, the gamma distortion index (GDI) is calculated with the following expression [32]:

$$GDI = AVG < |L_{i,on} - L_{i,off}| >_{i=0\sim255} \quad (2)$$

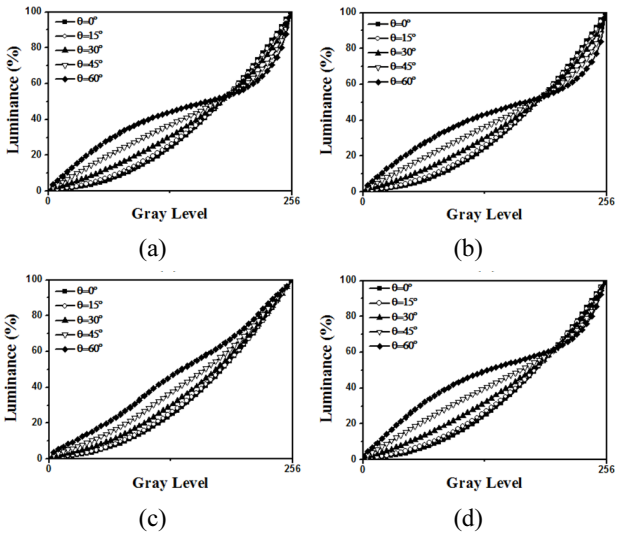

FIG. 7. Viewing-angle-dependent gamma curves at several polar viewing angles and fixed azimuthal angle 0°: (a) The conventional 4-domain case, (b) Case 1, (c) Case 2, and (d) Case 3.

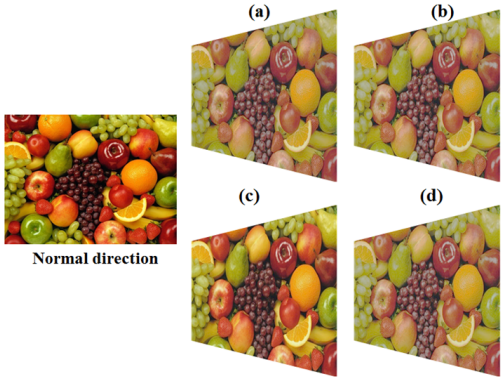

FIG. 8. Calculated images at normal viewing angle and oblique viewing angle with polar angle of 60° and azimuthal angle of 0°: (a) The conventional 4-domain case, (b) Case 1, (c) Case 2, and (d) Case 3.

where $L_{i,on}$ and $L_{i,off}$ denote luminance corresponding to the ith gray level on-axis and off-axis respectively, and $\langle\rangle$ denotes the average for all cases of arbitrary gray levels. A smaller value of *GDI* means better off-axis image quality. The calculated *GDI* for polar angle 30° (60°) is 4.25 (14.17) in the conventional 4-domain case, 4.50 (15.71) in case 1, and 4.08 (13.84) in case 3. These results imply the image quality of case 3 is more improved than the two other cases, while case 1 is even worse than the conventional 4-domain case. Remarkably, although the only difference of case 2 from case 1 is W_0 of the sub-region, the *GDI* of case 2 is reduced to 3.28 (23% less than the conventional 4-domain case) and 13.10 (8.1% less for polar angles of 30° and 60° respectively. Therefore, case 2 shows huge reduction in gamma distortion, and would display the best image quality among the proposed cases. Images along normal and oblique viewing directions are calculated to visualize the effects of the reduced *GDI* in the proposed 8-domain VA device, as shown in Fig. 8. As clearly indicated, the original image in the normal direction is best perceived in case 2 for the viewing-angle direction with polar angle of 60° at azimuthal angle of 0°, as compared to the other cases. These simulated images also demonstrate the outstanding effect of the proposed 8-domain, which is optimized with respect to pixel structure and anchoring energy.

IV. SUMMARY

We proposed an 8-domain PS-VA mode in which the main-region and sub-region have different widths and spacings of slits in their electrodes, and also the anchoring energies in each region have different amplitudes. The optimization of both parameters gave rise to lower gamma distortion index at oblique viewing angles than that of the 4-domain PS-VA, while keeping both high contrast ratio in the normal direction and the same transmittance as that of the 4-domain PS-VA. We believe the proposed design can contribute to the development of a PS-VA mode with high resolution, high image quality, and low power consumption.

ACKNOWLEDGMENT

This research was supported by Basic Science Research Program through the National Research Foundation of Korea (NRF) funded by Ministry of Education (2016R1A6A3A 11930056), 'The Cross-Ministry Giga KOREA Project' grant from the Ministry of Science, ICT and Future Planning, Korea, and the selection of research-oriented professor of Chonbuk National University in 2017.

REFERENCES

1. R. A. Soref, "Field effect in nematic liquid crystals obtained with interdigital electrodes," J. Appl. Phys. **45,** 5466-5468 (1974).
2. M. Oh-e and K. Kondo, "Electro-optical characteristics and switching behavior of the in-plane switching mode," Appl. Phys. Lett. **67**, 3895-3897 (1995).
3. S. H. Lee, S. L. Lee, and H. Y. Kim, "Electro-optic characteristics and switching principle of a nematic liquid crystal cell controlled by fringe-field switching," Appl. Phys. Lett. **73**, 2881-2883 (1998).
4. S. H. Hong, I. C. Park, H. Y. Kim, and S. H. Lee, "Electro-optic characteristic of fringe field switching mode depending on rubbing direction," Japan. J. Appl. Phys. **39**, L527-530 (2000).
5. S. H. Lee, S. M. Lee, H. Y. Kim, J. M. Kim, S. H. Hong, Y. H. Jeong, C. H. Park, Y. J. Choi, J. Y. Lee, J. W. Koh, and H. S. Park, "18.1"Ultra-FFS TFT-LCD with super image quality and fast response time," SID Int. Symp. Dig. Tech. Pap. **32**, 484-487 (2001).
6. A. Takeda, S. Kataoka, T. Sasaki, H. Chida, H. Tsuda, K. Ohmuro, T. Sasabayashi, Y. Koike, and K. Okamoto, "A super-high image quality multi-domain vertical alignment LCD by new rubbing-less technology," SID Int. Symp. Dig. Tech. Pap. **29**, 1077-1080 (1998).
7. K. H. Kim, K. Lee, S. B. Park, J. K. Song, S. N. Kim, and J. H. Souk, "Domain divided vertical alignment mode with optimized fringe field effect," in *Proc. of the 18th International Display Research Conference/Asia Display* (Sheraton Walker-Hill, Korea, Sept. 1998), pp. 383-386.
8. Y. Taniguchi, H. Inoue, M. Sawasaki, Y. Tanaka, T. Hasegawa, T. Sasaki, Y. Koike, and K. Okamoto, "An ulta-high-quality MVA-LCD using a new multi-layer CF resin spacer and black-matrix," SID Int. Symp. Dig. Tech. Pap. **31**, 378-381 (2000).
9. S. Kataoka, A. Takeda, H. Tsuda, Y. Koike, H. Inoue, T. Fujikawa, T. Sasabayashi, and K. Okamoto, "A new MVA-LCD with jagged shaped pixel electrodes," SID Int. Symp. Dig. Tech. Pap. **31**, 1066-1069 (2000).
10. Y. Yamada, K. Miyachi, M. Kubo, S. Mizushima, Y. Ishii, and M. Hijikigawa, "Fast response and wide-viewing angle technologies for LC-TV application," 9th Int. Display Work-

shops (Hiroshima, Japan). 203-206 (2002).
11. M. Yoshiga, M. Fukumoto, Y. Hamawaki, T. Unate, and T. Sunata, "Control of the LC orientation in a vertical aligned AMLCD with didived domains," 7th Int. Display Workshops (Kobe, Japan). 211-214 (2000).
12. K. H. Kim, J. J. Ryu, S. B. Park, J. K. Song, B. W. Lee, J. S. Byun, and J. H. Souk, "Current status and advance in PVA technology for high performance LCD monitor application," 1st Int. Meeting on Information Display (Daegu, Korea). 58-61 (2001).
13. S. I. Jun, W. Y. Park, I. G. Kim, J. Y. Lee, and J. H. Souk, "Panel transmittance analysis of PVA mode and a nobel pixel design," SID Int. Symp. Dig. Tech. Pap. **33**, 208-211 (2002).
14. Y. Kume, N. Yamada, S. Kozaki, H. Kishishita, F. Funada, and M. Hijikigawa, "Advanced ASM mode (Axially symmetric aligned microcell mode): Improvement of display performances by using negative dielectric liquid crystal," SID Int. Symp. Dig. Tech. Pap. **29**, 1089-1092 (1998).
15. S. G. Kim, S. M. Kim, Y. S. Kim, H. K. Lee, and S. H. Lee, "Stabilization of the liquid crystal director in the patterned vertical alignment mode through formation of pretilt angle by reactive mesogen," Appl. Phys. Lett. **90**, 261910 (2007).
16. S. M. Kim, I. Y. Cho, W. I. Kim, K. U. Jeong, S. H. Lee, G. D. Lee, J. Son, J. J. Lyu, and K. H. Kim, "Surface-modification on vertical alignment layer using UV-curable reactive mesogens," Japan. J. Appl. Phys. **48**, 032405 (2009).
17. R. Lu, S. T. Wu, and S. H. Lee, "Reducing the color shift if a multidomain vertical alignment liquid crystal display using dual threshold voltages," Appl. Phys. Lett. **92**, 051114 (2008).
18. K. H. Kim, N. D. Kim, D. G. Kim, S. Y. Kim, J. H. Park, S. S. Seomun, B. H. Berkeley, and S. S. Kim, "A 57-in. wide UXGA TFT-LCD for HDTV application," SID Int. Symp. Dig. Tech. Pap. **35**, 106-109 (2004).
19. S. S. Kim, "Super PVA sets new state-of-the-art for LCD-TV," SID Int. Symp. Dig. Tech. Pap. **35**, 760-763 (2004).
20. S. S. Kim, B. H. Berkeley, K. H. Kim, and J. K. Song, "New technologies for advanced LCD-TV performance," J. Soc. Inf. Disp. **12/4**, 760-763 (2004).
21. S. S. Kim, "The world's Largest (82-in.) TFT-LCD," SID Int. Symp. Dig. Tech. Pap. **36**, 1842-1847 (2005).
22. S. B. Park, J. J. Lyu, Y. S. Um, H. W. Do, S. N. Ahn, K. W. Choi, K. H. Kim, and S. S. Kim, "A novel charge-shared S-PVA technology," SID Int. Symp. Dig. Tech. Pap. **36**, 1252-1254 (2007).
23. Y. P. Huang, W. K. Huang, C. H. Tsao, J. J. Su, H. L. Hou, L. Liao, C. Y. Lee, T. R. Chang, Y. C. Lin, and P. L. Chen, "Additional refresh technology (ART) of advanced-MVA (AMVA) mode for high quality LCDs," SID Int. Symp. Dig. Tech. Pap. **38**, 1010-1013 (2007).
24. S. S. Kim, B. H. Berkeley, and T. Kim, "Advancements for highest-performance LCD-TV," SID Int. Symp. Dig. Tech. Pap. **37**, 1938-1941 (2006).
25. S. S. Kim, B. H. You, J. H. Cho, D. G. Kim, B. H. Berkeley, and N. D. Kim, "An 82-in. ultra-definition 120-Hz LCD TV using new driving scheme and advanced Super PVA technology," J. Soc. Inf. Disp. **17/2**, 71-78 (2009).
26. S. J. Kim, K. C. Shin, H. Kim, H. G. Oh, J. Jung, and H. S. Kim, "Development of a resistivity division driving method for the vertically placed RGB pixels of the eight-domain thin-film-transistors liquid crystal display," J. Inf. Disp. **14**, 93-96 (2013).
27. X. Nie, R. Lu, H. Xianyu, T. X. Wu, and S. T. Wu, "Anchoring energy and cell gap effects on liquid crystal response time," J. Appl. Phys. **101**, 103110 (2007).
28. J. H. Kim, W. S. Kang, H. S. Choi, K. Park, J. H. Lee, S. Yoon, S. Yoon, G. D. Lee, and S. H. Lee, "Effect of surface anchoring energy on electro-optic characteristics of a fringe-field switching liquid crystal cell," J. Phys. D: Appl. Phys. **48**, 465506 (2015).
29. K. Hanaoka, Y. Nakanishi, Y. Inoue, S. Tanuma, Y. Koike, and K. A. Okamoto, "A new MVA-LCD by polymer sustained alignment technology," SID Int. Symp. Dig. Tech. Pap. **35**, 1200-1203 (2004).
30. K. Takatoh, M. Hasegawa, M. Koden, N. Itoh, R. Hasegawa, and M. Sakamoto, "Alignment technologies and applications of liquid crystal devices," Liquid Crystals Book Series (London: Taylor & Francis) Chapter 2.2.3, Alignment mechanisms. 30-32 (2005).
31. M. Stokes, M. Anderson, S. Chandrasekar, and R. Motta, "A standard default color space for the internet: sRGB 4th IS&T/SID Color Imaging," Conf. (Arizona,USA). 238-246 (1992).
32. B. J. Mun, T. Y. Jin, G. D. Lee, Y. J. Lim, and S. H. Lee, "Optical approach to improve the γ curve in a vertical-alignment liquid-crystal cell," Opt. Lett. **38**, 799-801 (2013).